Control of the Morphology and Size of PbS Nanowires Using Gold Nanoparticles

Ken-Tye Yong,[†,‡] Yudhisthira Sahoo,[†,§] Kaushik Roy Choudhury,[†,||] Mark T. Swihart,*[,†,‡] John R. Minter,[⊥] and Paras N. Prasad*[,†,§,||]

Institute for Lasers, Photonics and Biophotonics, Department of Chemical and Biological Engineering, Department of Chemistry, and Department of Physics, University at Buffalo, The State University of New York, Buffalo, New York 14260-4200, and Foundation Science and Technology Center, Eastman Kodak Company Research Laboratories, Rochester, New York 14650

Received July 28, 2006. Revised Manuscript Received September 25, 2006

Anisotropic growth of nanocrystalline PbS with a variety of morphologies was achieved via hot colloidal synthesis in the presence of Au nanoparticles. Synthesis using Au nanoparticles produced more uniform diameter nanowires than could be obtained in their absence. A variety of other morphologies, such as nanorods, nanocubes, nanocauliflowers, and core−shell particles, were also obtained by varying the molar ratios of the precursor ions. The effect of Au seed particles appears to result from their ability to provide nucleation sites to seed anisotropic growth of the semiconductor nanocrystals. The method demonstrated here provides a facile hot colloidal method of producing high-quality high-aspect-ratio PbS nanowires of controlled diameter in high yield. The ability of these nanowires to provide infrared photosensitization in a polymeric photoconductive device is demonstrated.

Introduction

Synthetic control of the morphology of semiconductor nanocrystals is an ongoing research focus in the field of materials chemistry because of the influence of shape and texture, via quantum confinement, on the optoelectronic properties of these structures.[1] Many recent efforts have focused on low-dimensional structures (e.g., nanowires (NWs) and nanorods) of metal and semiconductor materials.[2] There have been numerous reports on growth strategies for nonspherical CdSe,[3] CdTe,[4] CdS,[5,6] and Pb[7] in solution and for Si, Ge, InP, CdS, and ZnS NWs via vapor-phase deposition.[8−11] CdSe and PbSe NWs have been prepared in solution in the presence of metallic seed particles, and their growth was interpreted in terms of a solution−liquid−solid (SLS) mechanism.[12−14] This approach was first applied to III−V materials and continues to be developed for those systems[15−22] as well as for group IV semiconductors.[23−25] More recently, CdTe,[26] CdSe,[27] ZnS,[28] and PbSe[29] nanowires have been fabricated via an oriented attachment process. The process involves the formation of wirelike aggregates resulting from dipole−dipole interaction between polar semicon-

* To whom correspondence should be addressed. E-mail: swihart@eng.buffalo.edu (M.T.S.); pnprasad@buffalo.edu (P.N.P.).

[†] Institute for Lasers, Photonics and Biophotonics, University at Buffalo, The State University of New York.

[‡] Department of Chemical and Biological Engineering, University at Buffalo, The State University of New York.

[§] Department of Chemistry, University at Buffalo, The State University of New York.

[||] Department of Physics, University at Buffalo, The State University of New York.

[⊥] Eastman Kodak Company Research Laboratories.

(1) Prasad, P. N. *Nanophotonics*; Wiley-Interscience: New York, 2004.
(2) Burda, C.; Chen, X.; Narayanan, R.; El-Sayed, M. A. *Chem. Rev.* **2005**, *105*, 1025.
(3) Manna, L.; Scher, E. C.; Alivisatos, A. P. *J. Am. Chem. Soc.* **2000**, *122*, 12700.
(4) Manna, L.; Milliron, D.; Meisel, A.; Scher, E. C.; Alivisatos, A. P. *Nat. Mater.* **2003**, *2*, 382−385.
(5) Jun, Y.-W.; Lee, S.-M.; Kang, N.-J.; Cheon, J. *J. Am. Chem. Soc.* **2001**, *123*, 5150.
(6) Gao, F.; Lu, Q.; Xie, S.; Zhao, D. *Adv. Mater.* **2002**, *14*, 1537.
(7) Wang, Y.; Jiang, X.; Herricks, T.; Xia, Y. *J. Phys. Chem. B.* **2004**, *108*, 8631.
(8) Morales, A. M.; Lieber, C. M. *Science* **1998**, *279*, 208.
(9) Barrelet, C. J.; Wu, Y.; Bell, D. C.; Lieber, C. M. *J. Am. Chem. Soc.* **2003**, *125*, 11498.
(10) Duan, X. F.; Huang, Y.; Cui, Y.; Wang, J. F.; Lieber, C. M. *Nature* **2001**, *409*, 66.
(11) Gudiksen, M. S.; Wang, J.; Lieber, C. M. *J. Phys. Chem. B* **2001**, *105*, 4062.
(12) Yu, H.; Li, J. B.; Loomis, R. A.; Gibbons, P. C.; Wang, L. W.; Buhro, W. E. *J. Am. Chem. Soc.* **2003**, *125*, 16168.
(13) Grebinski, J. W.; Hull, K. L.; Zhang, J.; Kosel, T. H.; Kuno, M. *Chem. Mater.* **2004**, *16*, 5260.
(14) Hull, K. L.; Grebinski, J. W.; Kosel, T. H.; Kuno, M. *Chem. Mater.* **2005**, *17*, 4416.
(15) Trentler, T. J.; Hickman, K. M.; Goel, S. C.; Viano, A. M.; Givvons, P. C.; Buhro, W. E. *Science* **1995**, *270*, 1791.
(16) Trentler, T. J.; Goel, S. C.; Hickman, K. M.; Viano, A. M.; Chiang, M. Y.; Beatty, A. M.; Gibbons, P. C.; Buhro, W. E. *J. Am. Chem. Soc.* **1997**, *119*, 2172.
(17) Yu, H.; Buhro, W. E. *Adv. Mater.* **2003**, *15*, 416.
(18) Yu, H.; Li, J. B.; Loomis, R. A.; Wang, L. W.; Buhro, W. E. *Nat. Mater.* **2003**, *2*, 517.
(19) Kan, S. H.; Aharoni, A.; Mokari, T.; Banin, U. *Faraday Discuss.* **2004**, *125*, 23.
(20) Kan, S. H.; Mokari, T.; Rothenberg, E.; Banin, U. *Nat. Mater.* **2003**, *2*, 155.
(21) Davidson, F. M., III; Wiacek, R.; Korgel, B. A. *Chem. Mater.* **2005**, *17*, 230.
(22) Nedeljkovic, J. M.; Micic, O. I.; Ahrenkiel, S. P.; Miedaner, A.; Nozik, A. J. *J. Am. Chem. Soc.* **2004**, *126*, 2632.
(23) Holmes, J. D.; Johnston, K. P.; Doty, R. C.; Korgel, B. A. *Science* **2000**, *287*, 1471.
(24) Hanrath, T.; Korgel, B. A. *J. Am. Chem. Soc.* **2002**, *124*, 1424.
(25) Lu, X.; Fanfair, D. D.; Johnston, K. P.; Korgel, B. A. *J. Am. Chem. Soc.* **2005**, *127*, 15718.
(26) Tang, Z.; Kotov, N. A.; Giersig, M. *Science* **2002**, *297*, 237.
(27) Pradhan, N.; Xu, H.; Peng, X. *Nano Lett.* **2006**, *6*, 720.
(28) Yu, J. H.; Joo, J.; Park, H. M.; Baik, S.-I.; Kim, Y. W.; Kim, S. C.; Hyeon, T. *J. Am. Chem. Soc.* **2005**, *127*, 5662.
(29) Cho, K.-S.; Talapin, D. V.; Gaschler, W.; Murray, C. B. *J. Am. Chem. Soc.* **2005**, *127*, 7140.

10.1021/cm061771q CCC: $33.50
Published on Web 11/16/2006

ductor nanoparticles. In a stoichiometric nanocrystal of any of these compound semiconductor materials, some faces will be terminated with the cation and others with the anion. This creates a net dipole moment on each particle that tends to orient the particles in a common direction. These examples indicate that the development of facile, effective, and straightforward methods of creating novel nanoarchitectures of semiconductors is an important goal from both scientific and technological perspectives.

Lead sulfide (PbS) is a narrow band gap semiconductor with a bulk band gap energy of 0.41 eV and a large exciton Bohr radius of 18 nm,[1] which makes it well-suited for use in IR detectors.[30] A variety of morphologies of PbS NCs have been reported recently. For example, rodlike PbS NCs were produced using a combination of a surfactant and polymer matrix as the template.[31] Closed PbS nanowires (PbS CNWs) in the shape of ellipses and parallelograms were synthesized in the presence of poly[*N*-(2-aminoethyl)acrylamide] in ethylenediamine/H_2O solution.[32] PbS dendrites composed of nanorods were fabricated through a hydrothermal process in the presence of *N*-cetyl-*N*,*N*,*N*-trimethylammonium bromide (CTAB).[33] Uniform cube-shaped PbS nanocrystals with particle sizes ranging from 6 to 13 nm can be prepared through a hot colloidal synthesis method.[34]

Semiconductor nanowires (NWs) represent a new class of nanoscale building blocks that have been used in electronic and photonic applications, including light-emitting diodes,[10] photodetectors,[35] and lasers.[36] Critical parameters that determine the properties and behavior of NWs are their crystallinity, stoichiometry, and size.[9] Though semiconductor nanowires of several semiconductors have been produced either by vapor- or solution-based methodologies, there has not been a reliable method of producing high-quality PbS NWs of controlled size in solution. Recently, Wang and coworkers[37] presented a surfactant-assisted solvothermal approach to synthesize PbS nanotubes, nanorods, and nanowires at low temperature (85 °C), with a low yield of NWs. Ge et al.[38] prepared orthogonal PbS NW arrays by a chemical vapor deposition method. In this paper, we report the first anisotropic growth of colloidal PbS NWs by seeding with Au nanoparticles. Multi-micrometer-long wirelike structures, with controlled diameters, can be produced using this approach. By systematically varying the synthetic parameters, we were able to controllably produce nanorod, nanocube, nanocauliflower, and core−shell morphologies and high-quality crystalline nanowires with a narrow distribution of diameters.

Materials and Methods

Materials. Lead oxide (PbO), oleic acid, 1-hexadecylamine, sulfur, trioctylphosphine (TOP), tetraoctylammonium bromide (98%) (TOAB), hydrogen tetrachloroaurate(III) trihydrate ($HAuCl_4 \cdot 3H_2O$), sodium borohydride, dodecylamine, and phenyl ether were purchased from Aldrich. All chemicals were used as received. All solvents (hexane, toluene, and acetone) were used without further purification.

Synthesis of Au Nanoparticles. Gold nanoparticles were prepared following Brust's two-phase method.[39] Twenty milliliters of 5 mM $HAuCl_4$ solution was mixed with 10 mL of a 25 mM TOAB toluene solution. The mixture was vigorously stirred for 15 min. Two immiscible layers immediately formed, with an orange/red organic phase on top and the clear/slightly orange tinted aqueous phase on the bottom. The organic phase was separated into a glass vial and a solution of 0.12 g of dodecylamine in 5 mL of toluene was added, followed by dropwise addition of 5 mL of 0.1 M sodium borohydride aqueous solution to the stirring reaction mixture. An instantaneous color change of the organic phase was observed, from orange-red to a deep red color. Stirring was continued for 30 min, then the organic phase containing gold nanoparticles was separated from the aqueous phase, and the organic phase was adjusted to 20 mL by the addition of toluene. In general, these particles were easily dispersible in toluene, chloroform, and tetrahydrofuran (THF) and could be repeatedly precipitated and redispersed. The average diameter of the gold nanoparticles (NPs) was $\sim 4 \pm 1.2$ nm. Although the Au NPs were stabilized (capped) with dodecylamine during synthesis, during the subsequent PbS growth, they are heated in the presence of a large excess of hexadecylamine and TOP. Thus, ligand exchange under growth conditions is likely. Presumably, ligand desoprtion is necessary for PbS nucleation on the seed particles, and therefore more strongly bound capping agents, such as thiols, were not used.

Synthesis of PbS Nanowires (NWs). A 1.0 M stock solution of trioctylphosphine sulfur (TOP−S) was prepared in advance, by dissolving 1.6 g of sulfur in 50 mL of TOP. Two millimoles of lead oxide, 2 mmol of hexadecylamine, Au nanoparticles corresponding to ~0.025 mmol of metal atoms, and 1.5 mL of oleic acid were dissolved in 5 mL of phenyl ether. The reaction mixture was heated to ~200 °C for ~15−30 min under an argon flow. Subsequently, 2 mL of 1.0 M TOP−S solution was injected into the hot (~200 °C) reaction mixture. The reaction mixture was held at ~200 °C for 1 h, and then an aliquot was removed via syringe and was injected into a large volume of toluene at room temperature, thereby quenching any further growth of the NWs. The NWs were separated from the toluene solution by addition of ethanol and then centrifugation.

Synthesis of PbS Nanorods and Nanocubes. Lead oxide (0.5 mmol), 2 mmol of hexadecylamine, Au nanoparticles corresponding to ~0.025 mmol of metal atoms, and 1.5 mL of oleic acid were dissolved in 5 mL of phenyl ether. The reaction mixture was heated to 200 °C for ~15−30 min under an argon flow, and then 2 mL of 1.0 M TOP−S solution was injected with gentle stirring into the hot (200 °C) reaction mixture. The reaction mixture was held at ~200 °C for 1 h. The nanocrystals were then quenched and separated as described above for nanowires.

Synthesis of PbS "Nanocauliflower" Structures. Typically, 2 mmol of lead oxide, 2 mmol of hexadecylamine, freshly prepared gold nanoparticles corresponding to ~0.05 mmol of metal atoms, and 1 mL of oleic acid were dissolved in 7 mL of phenyl ether. The reaction mixture was heated to 200 °C for ~15−30 min under

(30) Gadenne, P.; Yagil, Y.; Deutscher, G. *J. Appl. Phys.* **1989**, *66*, 3019.
(31) Wang, S.; Yang, S. *Langmuir* **2000**, *16*, 389.
(32) Yu, D.; Wang, D.; Meng, Z.; Lu, J.; Qian, Y. *J. Mater. Chem.* **2002**, *12*, 403.
(33) Kuang, D.; Xu, A.; Fang, Y.; Liu, H.; Frommen, C.; Fenske, D. *Adv. Mater.* **2003**, *15*, 1747.
(34) Joo, J.; Na, H. B.; Yu, T.; Yu, J. H.; Kim, Y. W.; Wu, F.; Zhang, J. Z.; Hyeon, T. *J. Am. Chem. Soc.* **2003**, *125*, 11100.
(35) Wang, J. F.; Gudiksen, M. S.; Duan, X. F.; Cui, Y.; Lieber, C. M. *Science* **2001**, *293*, 1455.
(36) Duan, X. F.; Huang, Y.; Agarwal, R.; Lieber, C. M. *Nature* **2003**, *421*, 241.
(37) Zhang, C.; Kang, Z.; Shen, E.; Wang, E.; Gao, L.; Luo, F.; Tian, C.; Wang, C.; Lan, Y.; Li, J.; Cao, X. *J. Phys. Chem. B* **2006**, *110*, 184.
(38) Ge, J. P.; Wang, J.; Zhang, H.-X.; Wang, X.; Peng, Q.; Li, Y.-D. *Chem. Eur. J. A* **2005**, *11*, 1889.
(39) Brust, M.; Walker, M.; Bethell, D.; Schiffrin, D. J.; Whyman, R. *J. Chem. Soc., Chem. Commun.* **1994**, 801.

an argon flow. After that, 2 mL of 1.0 M TOP−S solution was injected under gentle stirring into the hot (200 °C) reaction mixture. The reaction mixture was held at ∼200 °C for 1 h. The nanocrystals were then quenched and separated as described above for nanowires.

Synthesis of Au−PbS Core−Shell NCs. One millimole of lead oxide, 1 mmol of hexadecylamine, freshly prepared gold nanoparticles corresponding to ∼0.05 mmol of metal atoms, and 1 mL of oleic acid were dissolved in 15 mL of phenyl ether. The reaction mixture was heated to 220 °C for ∼20−30 min under an argon flow. After that, 2 mL of 1.0 M TOP−S solution was injected under gentle stirring into the hot (220 °C) reaction mixture. The reaction mixture was held at ∼200 °C for 1 h. The nanocrystals were then quenched and separated as described above for nanowires.

Characterization Methods. *(i) Transmission Electron Microscopy.* Transmission electron microscopy (TEM) images were obtained using a JEOL model JEM-100CX microscope at an acceleration voltage of 80 kV. The specimens were prepared by drop-coating the sample dispersion onto an ultrathin carbon-coated copper grid, which was placed on filter paper to absorb excess solvent. High-resolution transmission electron microscopy (TEM) images were obtained with a model 200 JEOL microscope at an acceleration voltage of 200 kV.

(ii) Scanning Electron Microscopy. Scanning electron microscopy (SEM) images were obtained using an Hitachi S4000 field emission microscope at an acceleration voltage of 25 kV.

(iii) X-ray Diffraction (XRD). X-ray powder diffraction patterns were recorded using a Siemens D500 diffractometer, with Cu Kα radiation. A concentrated nanocrystal dispersion was drop-cast onto a quartz plate for measurement.

Results and Discussion

PbS NWs were produced, as described above, upon injecting trioctylphosphine sulfur (TOP−S) into a hot (∼200 °C) reaction mixture containing lead oleate, hexadecylamine, oleic acid, and ∼4 nm diameter gold nanoparticles. The morphology and size of the PbS NWs strongly depended on the concentration of the Au particles, composition of stabilizing agents, and the Pb to S molar ratio in the growth solution. With use of Pb:S:Au atomic ratios of 80:80:1 (0.025 mmol of Au and 2 mmol each of Pb and S), straight NWs were obtained as a mixture of individual wires and bundles. Separate batches with median diameters of ∼16 and ∼35 nm were produced by varying the heating time after TOP−S injection. Thinner NWs were produced upon aging the mixture for ∼16−20 min, rather than 1 h. Figure 1 shows TEM images of NWs with a median diameter of ∼35 nm and lengths from 3 to 10 μm. The TEM and HRTEM images demonstrate the high degree of crystallinity, slightly corrugated surfaces, and narrow diameter distribution of the NWs. In a typical reaction, approximately ∼170 mg of PbS nanowires were obtained using 2 mmol each of the lead and sulfur precursors, corresponding to ∼35% yield. The dimensions and structures of the PbS NWs change significantly as the metal nanoparticle concentration is changed. When the gold NP concentration was decreased from ∼0.025 to ∼0.0025 mmol of metal atoms, NWs with an average diameter of ∼57 nm were obtained. The surfaces of these thicker NWs exhibited sawlike structures as shown in Figure 2. In addition, a significant fraction of the nanowires were not straight, but exhibited random kinks and bends, such that they became entangled with one another. The sawlike

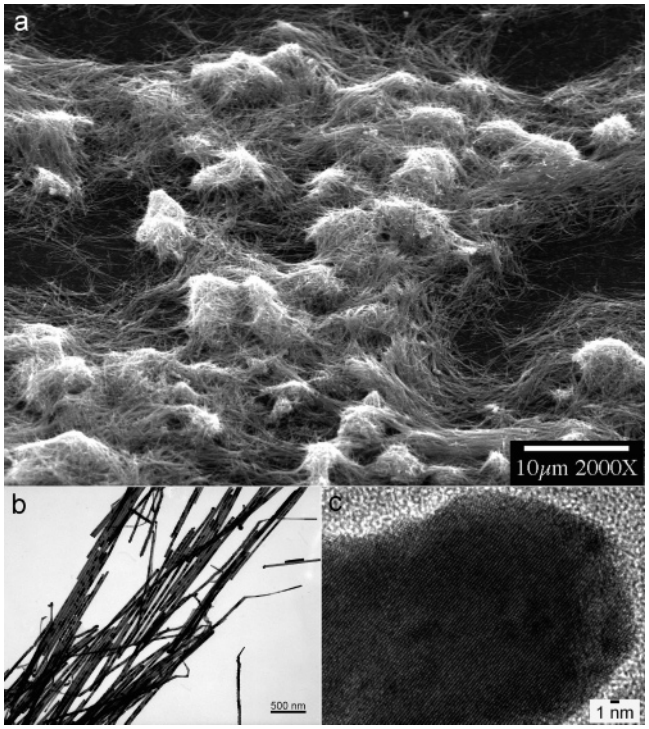

Figure 1. (a) SEM image of a large quantity of PbS NWs. (b) TEM image of PbS NWs showing that they are highly monodispersed in diameter. The average diameter of the NWs is 35 nm. The aspect ratio of the NWs is above 85. (c) HRTEM image of the end of a PbS NW, showing lattice fringes of 3.0 Å.

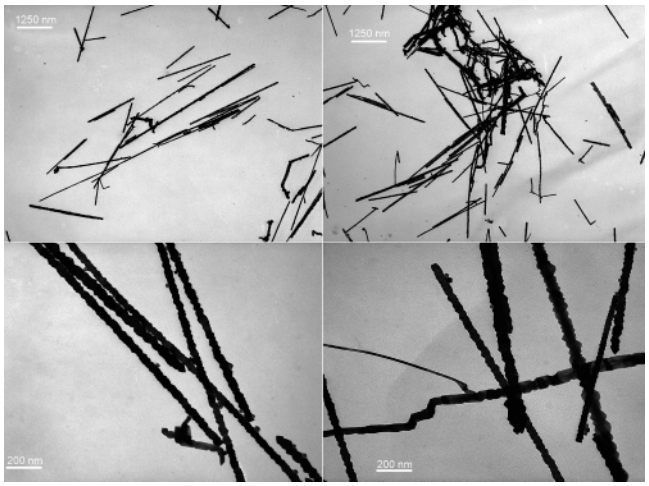

Figure 2. PbS NWs prepared in the presence of ∼0.0025 mmol of Au with a Pb:S ratio of 1:1. The average width of the NWs is ∼57 nm.

structure of the PbS NWs produced using this reduced concentration of Au NPs is somewhat similar to that of the PbSe NWs fabricated by the research groups of Murray[29] and Kuno.[14]

Along with the seed to precursor ratio, the Pb:S molar ratio also plays an important role in synthesizing straight NWs. Generally, straight, well-defined PbS NWs were obtained using a 1:1 Pb:S ratio in the presence of Au NPs corresponding to ∼0.025 mmol of metal atoms. Increasing the Pb:S ratio to 3:2 yielded straight individual and bundled PbS NWs with a larger average diameter of 55 nm (Figure 3). When the ratio was decreased to 1:4, no NWs were formed and instead rod- and cube-shaped PbS NCs were observed (see Figure 4). The population of PbS nanorods

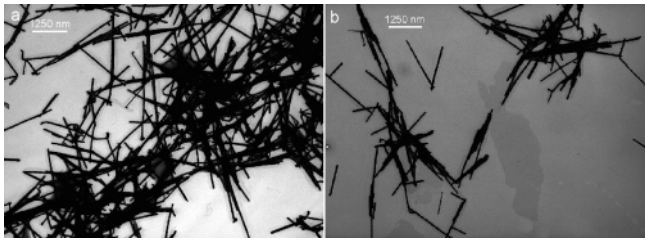

Figure 3. PbS NWs synthesized using a Pb:S ratio of 3:2. The average width of the NWs is ∼55 nm.

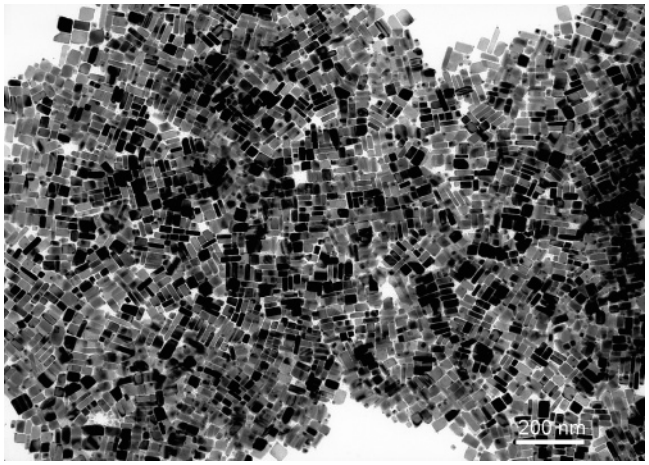

Figure 4. PbS nanorods (of square or rectangular cross section) and nanocubes prepared in the presence of ∼0.025 mmol of Au NPs, using a Pb:S ratio of 1:4.

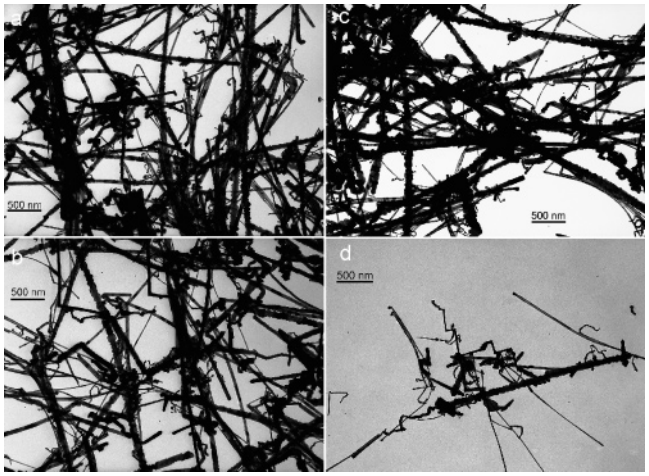

Figure 5. (a)−(d) PbS NWs prepared without using Au NPs.

and nanocubes is estimated to be 71% and 29%, respectively. Note that while we refer to the anisotropic structures in Figure 4 as nanorods, in fact we expect that their cross sections are not round, but square or rectangular. The nanorods have an average width and length of 12.2 and 48 nm, respectively. The nanocubes have an average edge length of 19.5 nm. Careful examination of the PbS nanorods and nanocubes reveals gold NPs embedded at one vertex of each nanocrystal.

To investigate whether straight NWs can be grown without Au NPs, control experiments were carried out at the same reaction conditions, but in the absence of Au NPs. In such experiments, NWs were obtained, but these wires displayed a noticeably different morphology (see Figure 5) with a high degree of polydispersity, irregular branched structures, and highly corrugated surfaces. There were also tentacle-like lateral growth features on the NWs. These NWs were highly agglomerated, compared to those produced using Au NP seeds. Figure 6 compares the diameter distributions obtained under identical reaction conditions, with and without Au NPs as seeds. The Au-seeded wires have a narrower size distribution and are much thinner than the unseeded NWs. The Au-seeded wires have an average diameter of ∼35 nm. The unseeded PbS NWs, on the other hand, are polydisperse and larger, with an average diameter of ∼55 nm. NW aggregation was observed in both cases. However, the degree of aggregation was much greater in the absence of Au NPs. It is clear from these experiments that although the presence of Au nanoparticles is not essential for the formation of PbS NWs, it has tremendous effects on the morphology and size of the NWs.

The structure of the PbS NWs was further examined by powder X-ray diffraction (XRD). The diffractogram shown in Figure 7 is consistent with the bulk rock salt structure of PbS. The three strong peaks with 2θ values of 26.05, 30.15, and 43.15° correspond to the (111), (200), and (220) planes, respectively. The Au nanoparticle content is too low to show any characteristic XRD peaks, which would appear at 2θ values of 38.18, 44.39, and 64.57°. Figure 1b and Figure 8 show HRTEM images of different parts of the PbS NWs with average diameters of ∼16 and ∼35 nm, respectively. These images indicate that the NWs are crystalline; they exhibit well-resolved lattice fringes. The boundaries of the images suggest corrugated surfaces. The fringe spacing is estimated to be 0.30 nm, which corresponds to the [200] lattice spacing of PbS, indicating that [100] is the preferential growth direction for the wires. The selected area electron diffraction (SAED) pattern from a ∼16 nm PbS NW, shown in Figure 8a, confirms the rock salt crystal structure of PbS. The XRD, SAED, and the HRTEM results show that the long axis of the NWs corresponds to the [100] direction of the cubic rock salt structure. Additionally, we note that the diameter of NWs (∼16 nm) and nanorods (∼12 nm) shown in Figure 4 and Supporting Information are smaller than the Bohr excitonic radius in PbS (∼18 nm). The electrons and holes in these nanostructures should therefore exhibit quantum confinement in the directions perpendicular to the wire axis.

In addition to NWs, other interesting morphologies can be synthesized upon tuning the concentration of gold NPs and precursor concentrations and the volume of solvent. For instance, when the reaction was carried out with Au NPs corresponding to ∼0.05 mmol of Au atoms, using a Pb:S ratio of 1:1 (2 mmol of Pb and 2 mmol of S), 1.0 mL of oleic acid, and 7 mL of phenyl ether at 200 °C, "nanocauliflower" structures appeared. The "nanocauliflower" structures seen in Figure 9 contain more than 100 nanowires growing out from both sides of a central "stem", with diameters ranging from 20 to 50 nm and lengths up to 1 μm (see Figure S5). When the reaction was carried out with Au NPs corresponding to ∼0.05 mmol of Au atoms, using a Pb:S ratio of 1:2 (1 mmol of Pb and 2 mmol of S), 1.0 mL of oleic acid, and 15 mL of phenyl ether at 220 °C, gold−PbS core−shell structures were obtained. Figure 9c shows

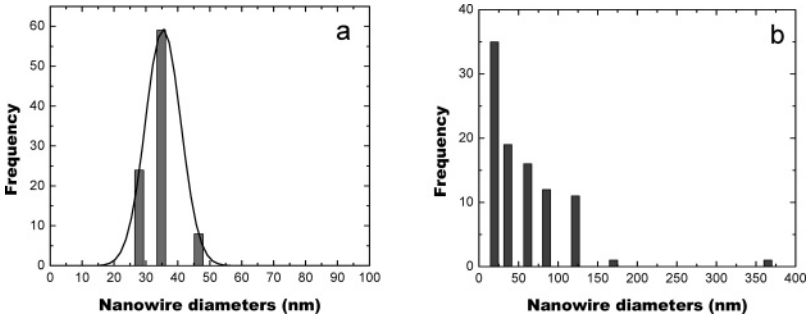

Figure 6. Diameter distributions of PbS NWs synthesized in the (a) presence and (b) absence of Au NPs. In (a) the mean diameter is 35 nm and the standard deviation is 4.9 nm. In (b) the distribution is far from Gaussian, and therefore the mean and standard deviation are not particularly meaningful.

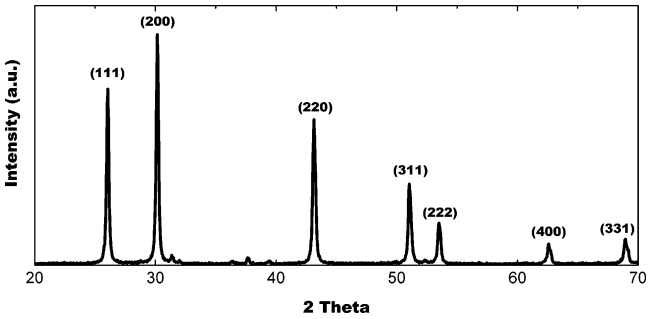

Figure 7. XRD pattern of PbS NWs like those shown in Figure 1.

TEM images of the Au core−PbS shell NPs. As shown there, various PbS shell morphologies were produced simultaneously, including spherical, cubic, and hexagonal shells. The Au−PbS core−shell NPs were relatively monodispersed in size. In these structures, the gold core diameter was at least 3 times that of the initial seed particles and thus had a volume equivalent to 25−30 seed particles. TEM analyses of the size of the Au−PbS core−shell particles showed the average core and shell diameters were 12 and 39 nm, respectively. Further analysis of the core−shell particles using EDS has confirmed the presence of Au (see Figure S6).

PbS NWs like those shown in Figure 5 can form by spontaneous alignment and fusion of PbS nanoparticles. TEM imaging has shown that the NWs consistently possess corrugated surfaces that can be attributed to (111) face defects from the oriented attachment of PbS particles along the ⟨100⟩ axis of the rock salt structure. Formation of such corrugated NWs of PbSe has been explained by Cho et al.[29] using a model based on dipolar interactions between nanoparticles. The origin of the dipole in that system was suggested to arise from various configurations for the stoichiometric termination of polar {111} faces. PbS, being isomorphic to PbSe, can exhibit similar polar termination of the {111} faces, leading to strong dipolar interactions between nanocrystals. We therefore suggest that the long corrugated NWs formed when Pb and S precursors are reacted alone (without Au seeding) result from the fusion of quasi-spherical (octahedral) particles possessing dipole moments due to the arrangement of their polar {111} faces. We find however that the presence of Au nanoparticles as seeds alters the dynamics, producing NWs that are more slender and less corrugated. To better illustrate the effects of Au NPs on the formation of PbS NWs, a diagram showing observed morphologies vs Pb:S ratio and gold nanoparticle concentration is presented in Figure 10. When appreciable amounts of Au NPs are used (∼0.025 mmol of metal atoms), straight NWs of uniform diameter are produced. Without Au seeding, the morphology degenerates to random aggregates of kinked NWs with a relatively broad distribution of diameters.

It appears that the introduction of Au nanoparticles shifts the nanowire formation mechanism from one dominated by dipole-driven oriented aggregation to one in which anisotropic solid-catalyzed growth plays an important role. In many cases, metal-seeded anisotropic growth of nanowires or nanorods has been explained by the solution−liquid−solid (SLS) mechanism.[25] This is an extension of the vapor−liquid−solid (VLS) mechanism[11,24] that is widely used for growth of wirelike structures from vapor-phase precursors. In both cases, one or more precursors dissolve in a metal seed particle (usually assumed to be a molten droplet) and are expelled at a small point from which the nanowire grows. The growth persists under a continuous cycle of precursor dissolution in the droplet and crystallization at the droplet surface. For the SLS mechanism to be operative, a miscible, low-melting Au−Pb−S alloy must be possible. Previous studies have clearly shown that 4 nm diameter Au nanocrystals will not melt at the temperature used in this study.[40] Au−Pb liquid solutions can form with a melting point as low as 213 °C, at a composition of 85 wt % Pb.[41] Upon freezing, this eutectic composition should split into $AuPb_3$ and Pb. However, in control experiments in which the Pb precursor was heated with the Au nanoparticles (in the absence of sulfur), there was no evidence of formation of $AuPb_3$ or any other intermetallic compounds. Au and S do not form binary solid solutions (though the metastable compound Au_2S can be produced). Up to about 1 wt % (5 atom %) S can dissolve in liquid Au, but this results in only about a 16 °C reduction in the Au melting point. Therefore, while a low-melting ternary alloy cannot be ruled out, it is highly unlikely that Au-seeded PbS NWs grow from a completely liquefied seed droplet at ∼200 °C. We therefore speculate that the essential role of the seed particle is simply to provide a low-energy interface for heterogeneous nucleation of the PbS nanocrystal.[40] We hypothesize that, initially, PbS NCs nucleate on each seed particle and grow anisotropically from it, and that these NCs can serve as a size template for further growth via oriented attachment of the PbS nanocrystals, leading to more uniform NW formation

(40) Yong, K.-T.; Sahoo, Y.; Choudhury, K. R.; Swihart, M. T.; Minter, J. R.; Prasad, P. N. *Nano Lett.* **2006**, *6*, 709.
(41) *Smithells Metals Reference Book*, 7th ed.; Brandes, E. A., Brook, G. B., Ed.; Butterworth-Heinemann: Boston, 1998.

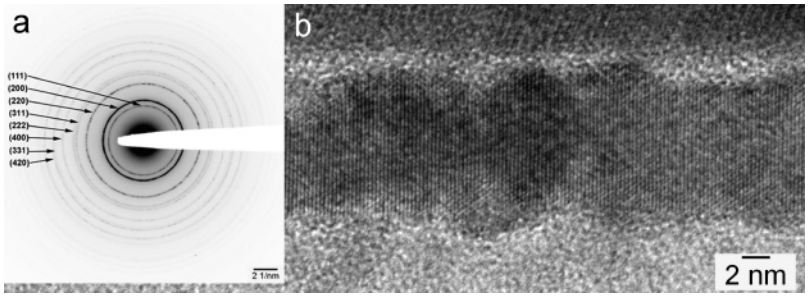

Figure 8. (a) Selected area electron diffraction (SAED) pattern from PbS NWs with average diameter of ~16 nm. (b) HRTEM image of a PbS NW with a diameter of ~16 nm.

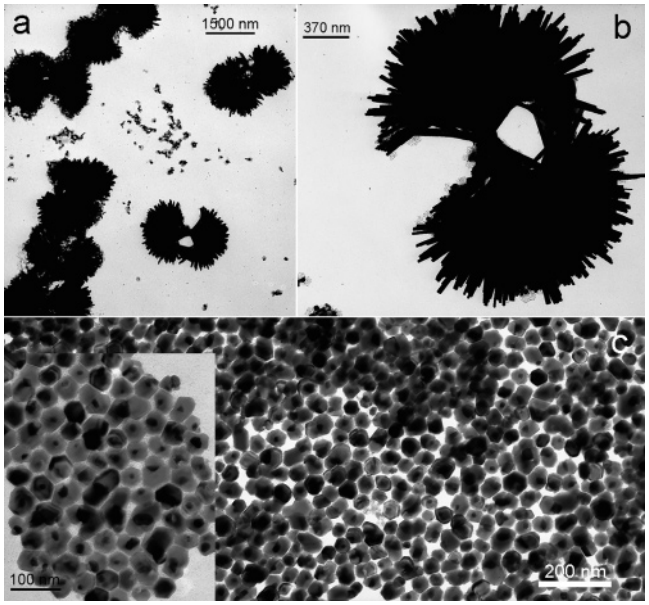

Figure 9. (a), (b) TEM images of PbS "nanocauliflower". (c) TEM images of gold core−PbS shell nanostructures. The inset shows a higher magnification on the core−shell nanostructures.

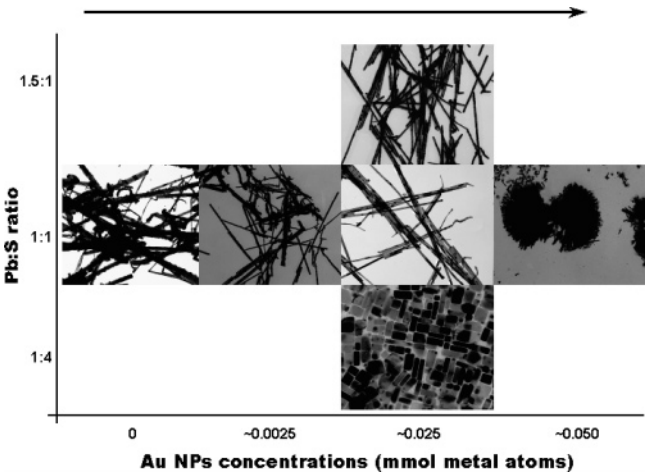

Figure 10. Diagram of observed morphology vs Pb:S ratio and Au nanoparticle concentration. Other small differences in synthesis parameters (e.g., total solvent volume) are not shown. For core−shell particles, several reaction parameters were changed, and that morphology is, therefore, not included in this diagram.

than occurs in the absence of Au seeding. This mechanistic picture, in which seeded anisotropic growth and oriented aggregation are both operative, is illustrated in Figure 11. Note that the "balls" observed at the end of some of the nanowires, which may be composed of pure Au, or may also contain Pb, S, or both, are much larger than the Au seed particles. We have previously observed the sintering of gold nanoparticles of this size in the presence of sulfur[42] at temperatures significantly lower than those used here. Thus, aggregation and sintering of the 4 nm Au particles to form larger ones is expected under the conditions used here.[13,14] This contrasts with our previous reports on the Au-seeded growth of PbSe,[40,42] and metal-seeded growth of CdSe,[43] in which sintering of seed particles was not observed under similar conditions, but in the absence of sulfur. Further details of the growth mechanisms operative under different reaction conditions in this system clearly remain a fruitful topic for further study.

The optical properties of PbS nanostructures can, in general, be adjusted by manipulating their dimension in a size range below the exciton Bohr radius. In nanowires, confinement in two dimensions, combined with high carrier mobility in the third dimension may allow, for example, highly efficient exciton generation and dissociation when a field is applied along the length of the nanowire. Straight PbS NWs of tunable diameter might therefore provide tunable optical and electronic properties that can enable new applications or enhance the performance of existing devices. To explore these possibilities, UV/vis/NIR absorbance spectroscopy was used to characterize the PbS NWs samples. However, neither the PbS NWs with ~16 nm diameter nor those with ~35 nm diameter showed any distinct maximum in the infrared (IR) region of their absorption spectrum. This lack of a sharp band-edge absorption feature may be due to the convolution of absorption peaks from NWs of different diameters, as well as to the lack of confinement in the axial dimension of the wire. Nonetheless, we have tested the PbS NWs in photodetector devices. It is now established that solution-processed polymeric devices with embedded semiconductor nanostructures (quantum dots, rods, multipods, and wires) have potential as platforms for low-cost, large-area versatile alternatives to their inorganic optoelectronic and photovoltaic counterparts.[44,45] Semiconductor NWs, with their inherent high mobilities and large aspect ratio, are good candidates for transporting charge carriers in such hybrid devices. We combined the PbS NWs (diameter ~16 nm) with the hole-conducting polymer poly(3-hexylthiophene)

(42) Shi, W.; Zeng, H.; Sahoo, Y.; Ohulchanskyy, T. Y.; Ding, Y.; Wang, Z. L.; Swihart, M. T.; Prasad, P. N. *Nano Lett.* **2006**, *6*, 875.
(43) Yong, K.-T.; Sahoo, Y.; Swihart, M. T.; Prasad, P. N. *Adv. Mater.* **2006**, *18*, 1978.
(44) Huynh, W. U.; Dittmer, J. J.; Alivisatos, A. P. *Science* **2002**, *295*, 2425.
(45) Gur, I.; Fromer, N. A.; Geier, M. L.; Alivisatos, A. P. *Science* **2005**, *310*, 462.

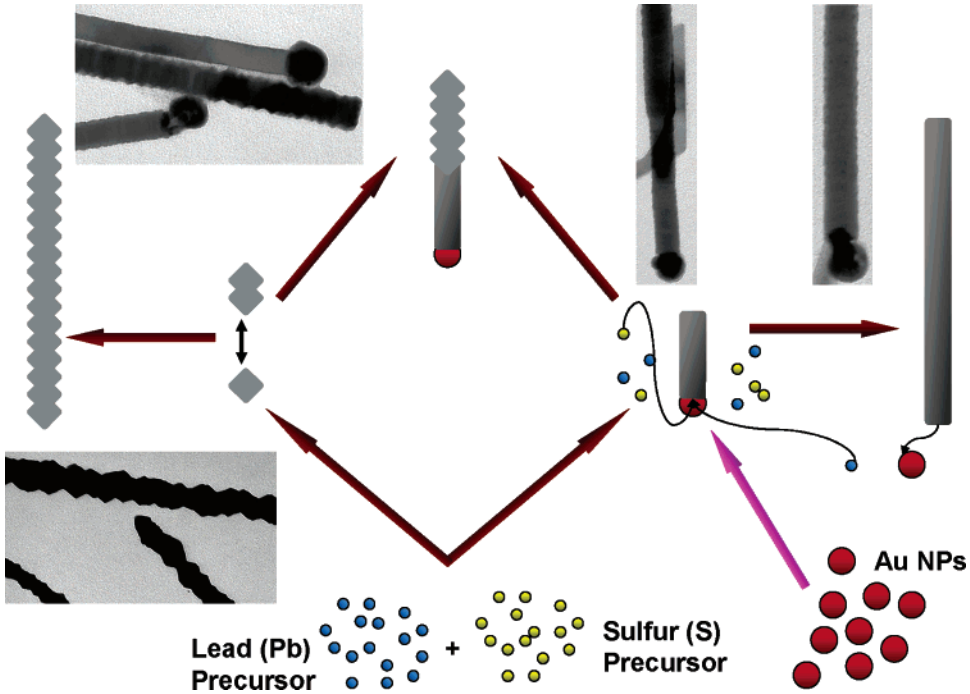

Figure 11. Schematic illustration of nanowire formation via simultaneous and competitive processes of seeded anisotropic growth (right) and oriented attachment (left). Inset TEM images show examples of the different observed morphologies associated with these different growth modes.

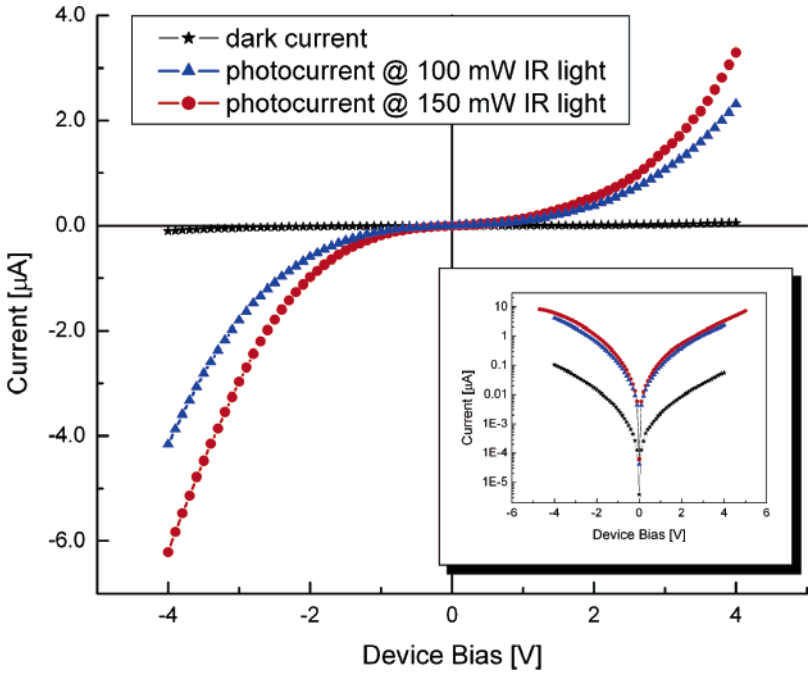

Figure 12. Dark and photocurrent of the polymer/nanowire device as a function of applied bias. The inset shows the same data on a semilog plot to emphasize the change in device current from dark to illuminated condition.

(P3HT) to produce infrared photoconductive devices containing ~10% NWs by weight, which could be easily cast as a thin film from chloroform solution. To enhance charge extraction, a layer of the organic semiconductor PEDOT:PSS was spin-coated on the ITO substrate before casting the active device. Details of the device fabrication process are included in the Supporting Information. A continuous-wave semiconductor laser operating at 1.34 μm was used to test the photoconducting nature of the composite. Figure 12 depicts the performance of the device under ambient conditions in the dark and when illuminated with infrared (IR) radiation. The device shows more than an order of magnitude enhancement of current when irradiated with IR light, indicating successful photosensitization of the polymer by the NWs. The photocurrent in the composite increases with increasing intensity of the incident radiation. At a maximum applied device bias of 4 V, the observed photocurrent results in a photogeneration quantum efficiency of $\sim 6 \times 10^{-4}$ charges per absorbed photon. Efforts are underway to optimize the device composition to enhance the photoconductive performance and also toward fabricating solution-processed NW transistors and photovoltaics.

Conclusions

The synthesis of high-quality, high-aspect-ratio crystalline PbS NWs of tunable diameter was achieved using Au NPs as seeds. Comparison of NWs prepared in the presence and absence of Au NPs illustrated the importance of the Au NPs in controlling the morphology of the synthesized NWs. The quality of the PbS NWs formed in the presence of Au NPs is superior to that of those obtained without Au NPs, apparently due to the ability of the Au seed particles to provide sites for heterogeneous nucleation and anisotropic growth of PbS nanocrystals. The optimum concentration range for PbS NW synthesis using 4 nm diameter Au NPs as seeds is ∼0.025 mmol of metal atoms in combination with 2 mmol each of Pb and S precursors in a total reaction volume of about 5 mL. Additional morphologies including nanocubes, nanorods, "nanocauliflower", and core−shell nanostructures were obtained by varying the Pb:S precursor ratio and the Au nanoparticle concentration.

Acknowledgment. This work was supported in part by the Chemistry and Life Sciences Directorate of the Air Force Office of Scientific Research (Grant #FA95550-06-1-0398).

Supporting Information Available: Procedure for preparing photoconductive devices. Additional SEM and TEM images of ∼35 nm diameter and ∼16 nm diameter nanowires. HRTEM images of ∼35 nm diameter nanowires. TEM image of nanocubes and nanorods. SEM image of nanocauliflower structures. EDS spectrum from gold core−PbS shell nanostructures. UV−vis−NIR absorbance spectra of nanowires and nanorods. This material is available free of charge via the Internet at http://pubs.acs.org.

CM061771Q